Metallaheteroborane Chemistry. Part 6.[1] Synthesis of *closo*-[2-(η-ligand)-1,2-$TeMB_{10}H_{10}$] Complexes with M(η-ligand) = $Rh(\eta^5\text{-}C_5Me_5)$ (1), $Ru(\eta^6\text{-}p\text{-}MeC_6H_4Pr^i)$ (2), $Ru(\eta^6\text{-}C_6Me_6)$ (3), and of *nido*-[6-(η^6-C_6Me_6)-8-(OEt)-6-RuB_9H_{12}] (4), their Characterisation by Nuclear Magnetic Resonance Spectroscopy and, for (1) and (3), by *X*-Ray Crystallography†

Faridoon, Marguerite McGrath, and Trevor R. Spalding*
Department of Chemistry, University College, Cork, Ireland
Xavier L. R. Fontaine, John D. Kennedy, and Mark Thornton-Pett
Department of Inorganic and Structural Chemistry, University of Leeds, Leeds LS2 9JT

The reaction between $[\{Rh(\eta^5\text{-}C_5Me_5)Cl_2\}_2]$ and *nido*-$[7\text{-}TeB_{10}H_{11}]^-$ in CH_2Cl_2 gave *closo*-[2-(η^5-C_5Me_5)-1,2-$TeRhB_{10}H_{10}$] (**1**) in moderate yield (65%). Similar reactions with $[\{Ru(\eta^6\text{-arene})Cl_2\}]_2$ (η^6-arene = p-$MeC_6H_4Pr^i$ or C_6Me_6) in CH_2Cl_2 gave *closo*-[2-(η^6-arene)-1,2-$TeRuB_{10}H_{10}$] complexes, (**2**) (40%) and (**3**) (60%) respectively. Reaction between $[\{Ru(\eta^6\text{-}C_6Me_6)Cl_2\}_2]$ and *nido*-$[7\text{-}TeB_{10}H_{11}]^-$ in EtOH produced *nido*-[6-(η^6-C_6Me_6)-8-(OEt)-6-RuB_9H_{12}] (**4**) in moderate yield (38%) together with (**3**) (15%). Compounds (**1**)—(**4**) were characterised by multielement n.m.r. spectroscopy and, for (**1**) and (**3**), by *X*-ray diffraction analyses. Crystals of (**1**) were orthorhombic, space group $P2_12_12_1$, $Z = 4$, $a = 988.3(1)$, $b = 1\,392.6(2)$, and $c = 2\,745.1(3)$ pm. The structure was refined to a final R of 0.0364 and R' of 0.0397 for the 3 637 reflections with $I \geqslant 1.5\sigma(I)$. There were two molecules in the asymmetric unit. Crystals of (**3**) were monoclinic, space group $C2/m$, $Z = 4$, $a = 1\,850.8(2)$, $b = 882.3(1)$, $c = 1\,216.5(1)$ pm, and $\beta = 100.84(1)°$. The structure was refined to a final R of 0.0286 and R' of 0.0403 for the 1 793 reflections with $I \geqslant 2.0\sigma(I)$. Both (**1**) and (**3**) contained closed $TeMB_{10}$ dodecahedra with Te and M adjacent. The metal tellurium distances were 252.9(4) and 253.6(4) pm in the two independent molecules of (**1**) and 254.9(2) in (**3**). Almost all comparable interatomic distances in the $MTeB_{10}$ cages of (**1**) and (**3**) were remarkably similar. Features in the bonding of the metals to the telluraborane and organic ligands are discussed in terms of the relevant molecular orbital interactions.

Compounds of the type $[\{M(\eta\text{-ligand})Cl_2\}_2]$, where M(η-ligand) is Ru(η^6-arene) or $Rh(\eta^5\text{-}C_5Me_5)$, have proved extremely useful starting substrates in the preparation of a wide variety of ruthena-[2] and rhoda-boranes.[3] This paper reports the use of these compounds to synthesize some metallatelluraboranes as part of our continuing studies of metallaheteroboranes.[1] We decided to prepare some twelve-vertex *closo*-(η^6-arene)ruthenatelluraboranes since such compounds are apparently unknown, although related complexes containing tellurium bonded to iron, cobalt,[4] rhodium,[5,6] iridium,[6] and platinum[7] have been reported. It was also of interest to prepare the closely related $Rh(\eta^5\text{-}C_5Me_5)$ compound which would provide us with data for a comparative study of the bonding-structure relationships in isoelectronic metal environments. In addition, the characterisation of the $Rh(\eta^5\text{-}C_5Me_5)$ compound would also provide data for a comparison with the *closo*-[2,2-$(PPh_3)_2$-2-H-1,2-$TeRhB_{10}H_{10}$] complex which has been described by us previously.[6]

During the present work we have also observed a ten-vertex *nido* reaction product which was formed by the excision of the tellurium atom from the telluraborane reagent *nido*-$[7\text{-}TeB_{10}H_{11}]^-$, the first such reaction to be observed in this type of system. It was formed as the major product when the reaction between $[\{Ru(\eta^6\text{-}C_6Me_6)Cl_2\}_2]$ and *nido*-$[7\text{-}TeB_{10}H_{11}]^-$ was carried out in ethanol whereas it was not observed when the reaction was carried out in dichloromethane, tetrahydrofuran (thf), or benzene. Diagrams (**I**)—(**III**) illustrate the cage numbering schemes for the compounds described in this paper.

Results and Discussion

Reaction between *nido*-$[7\text{-}TeB_{10}H_{11}]^-$ and the complexes $[\{M(\eta\text{-ligand})Cl_2\}_2]$ [where M(η-ligand) = $Rh(\eta^5\text{-}C_5Me_5)$, $Ru(\eta^6\text{-}p\text{-}MeC_6H_4Pr^i)$, or $Ru(\eta^6\text{-}C_6Me_6)$], in a 2:1 mole ratio in dichloromethane at room temperature for several days, gave air-stable *closo*-[2-(η-ligand)-1,2-$TeMB_{10}H_{10}$] compounds as the major products. These yellow compounds were isolated in moderate yields [M(η-ligand) = $Rh(\eta^5\text{-}C_5Me_5)$ (**1**), 65.0%; $Ru(\eta^6\text{-}p\text{-}MeC_6H_4Pr^i)$ (**2**), 40.1%; and $Ru(\eta^6\text{-}C_6Me_6)$ (**3**), 60.0%]. By contrast, when the reaction between $[\{Ru(\eta^6\text{-}C_6Me_6)Cl_2\}_2]$ and *nido*-$[7\text{-}TeB_{10}H_{11}]^-$ was carried out in refluxing ethanol for 1 h two products were formed. One of these was the *closo* compound (**3**) which was isolated in 14.9% yield and the other, which was orange, was found to be *nido*-[6-(η^6-C_6Me_6)-8-(OEt)-6-RuB_9H_{12}] (**4**) (38.2%). Compounds (**1**)—(**4**) were initially examined by i.r. spectroscopy. All showed absorptions in the B–H stretching region.

The molecular architectures of compounds (**1**) and (**3**) were established by single-crystal *X*-ray diffraction analyses. Suitable crystals of *closo*-[2-(η^5-C_5Me_5)-1,2-$TeRhB_{10}H_{10}$] were grown from CH_2Cl_2. They were orthorhombic, space group $P2_12_12_1$,

† 2-(η^5-Pentamethylcyclopentadienyl)-1-tellura-2-rhoda-*closo*-dodecaborane and 2-(η^6-hexamethylbenzene)-1-tellura-2-ruthena-*closo*-dodecaborane.

Supplementary data available: see Instructions for Authors, *J. Chem. Soc., Dalton Trans.*, 1990, Issue 1, pp. xix—xxii.

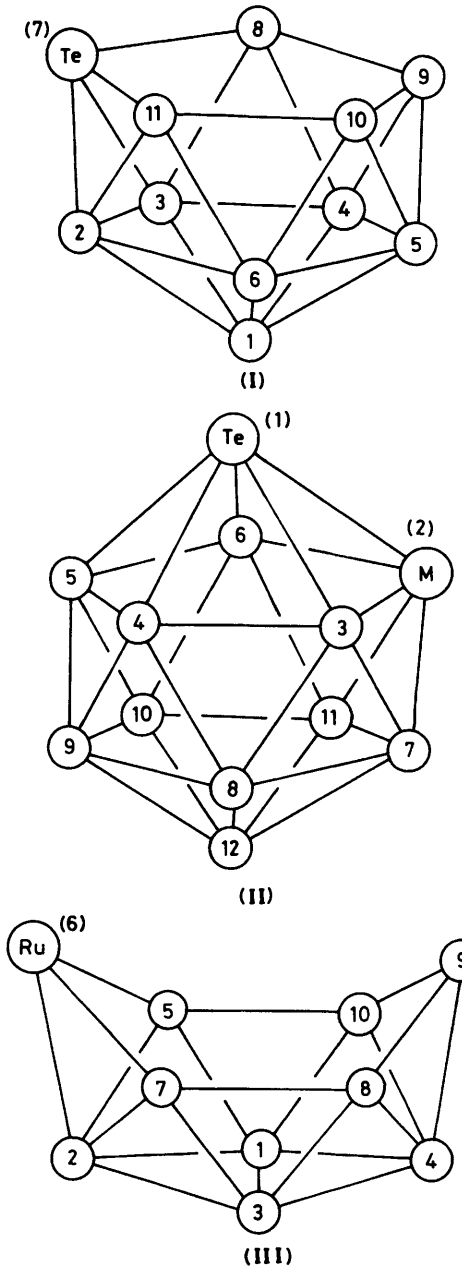

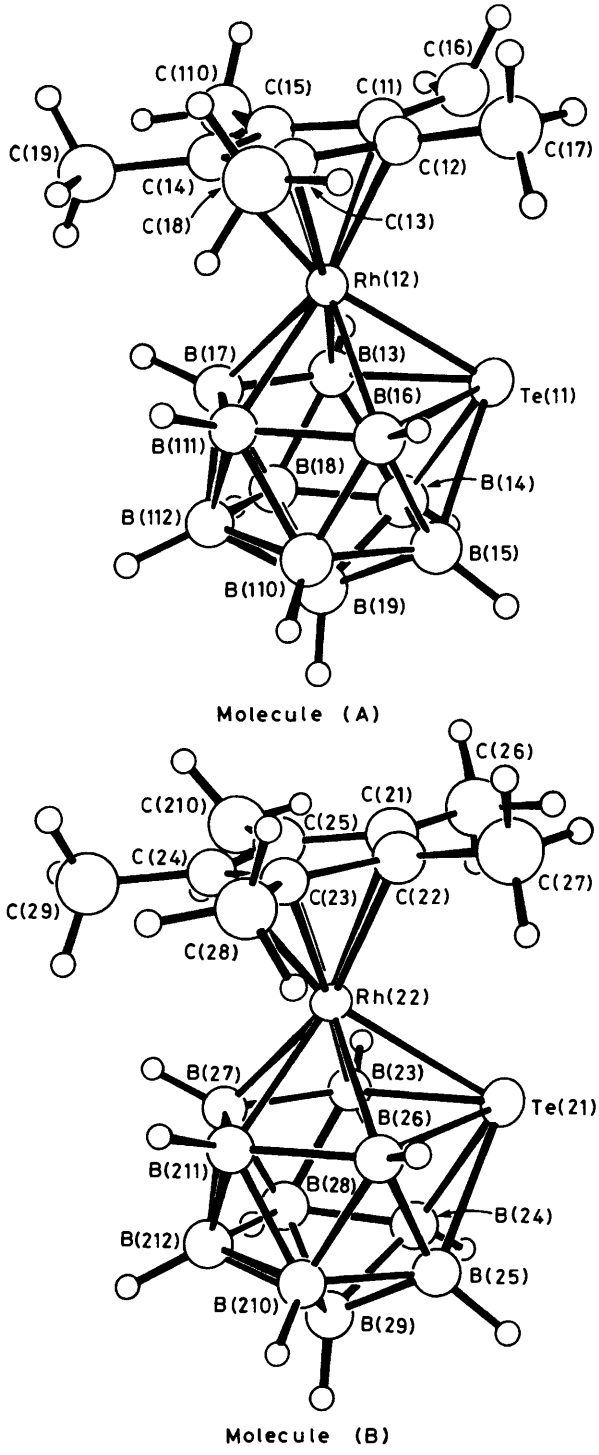

Figure 1. An ORTEP drawing of the molecular structure of *closo*-[2-(η^5-C_5Me_5)-1,2-$TeRhB_{10}H_{10}$] (**1**)

with two molecules in the asymmetric unit. Insufficient data were collectable to define accurately all the hydrogen-atom locations, but the CH_3 groups were fixed by using standard procedures, and *exo*-terminal boron-bound hydrogen atoms were located by using HYDEX potential-well calculations.[8] The molecules (A) and (B) are shown Figure 1, and selected interatomic distances and angles are given in Table 1. Like the other twelve-vertex *closo* rhodatelluraboranes whose structures have been reported, *i.e.* [2,2-$(PPh_3)_2$-2-H-1,2-$TeRhB_{10}H_{10}$] (**5**)[1] and the cycloboronated [2-(PPh_3)-2-H-2-($Ph_2PC_6H_4$)-1,2-$TeRhB_{10}H_{10}$] (**6**),[5] the cage contains adjacent rhodium and tellurium atoms. The Rh–Te distances in the two discrete molecules of (**1**) are 252.9(4) for (A) and 253.6(4) pm for (B), significantly shorter than the corresponding distances in (**5**) and (**6**) of 261.72(4) and 256.56(4) pm. The 'extra long' Rh–Te distance, in (**5**), correlates with the strong *trans* influence of the H ligand compared to the C_5Me_5 group in (**1**). In general the other distances between the cage atoms of compound (**1**) show the same trends as found previously in (**5**) and (**6**). For example there exist two 'long' Rh–B distances with mean values for (A) and (B) of Rh–B(3) 229.9(10) and Rh–B(6) 226.2(10) pm and two 'short' ones [mean values Rh–B(7) 220.1(10) and Rh–B(11) 220.8(10) pm]. Similar considerations apply to the Te–B interactions, Table 1. Boron–boron distances range from 172.4(17) to 198.2(17) pm in molecule (A) and from 173.5(16) to 196.7(16) in (B).

The η^5-C_5 ring atoms are essentially coplanar with a maxi-

Table 1. Selected interatomic distances (pm) and angles (°) for compound (**1**)

Molecule A		Molecule B	
(*i*) In the $RhTeB_{10}$ cage			
Rh(12)–Te(11)	252.9(4)	Rh(22)–Te(21)	253.6(4)
B(14)–Te(11)	226.4(13)	B(24)–Te(21)	231.6(12)
B(16)–Te(11)	239.3(12)	B(26)–Te(21)	238.0(12)
B(13)–Te(11)	240.7(12)	B(23)–Te(21)	239.2(12)
B(15)–Te(11)	226.7(12)	B(25)–Te(21)	230.2(13)
B(13)–Rh(12)	228.6(13)	B(23)–Rh(22)	231.2(12)
B(17)–Rh(22)	218.7(12)	B(27)–Rh(22)	221.4(11)
B(16)–Rh(12)	226.7(11)	B(26)–Rh(22)	225.9(12)
B(111)–Rh(12)	220.6(12)	B(211)–Rh(22)	220.9(11)
B(14)–B(13)	194.6(18)	B(24)–B(23)	196.7(16)
B(18)–B(13)	173.2(16)	B(28)–B(23)	176.9(16)
B(18)–B(14)	175.4(17)	B(28)–B(24)	173.5(16)
B(16)–B(15)	198.2(17)	B(26)–B(25)	194.7(16)
B(110)–B(15)	176.5(17)	B(210)–B(25)	175.4(16)
B(111)–B(16)	182.5(15)	B(211)–B(26)	181.0(15)
B(111)–B(17)	180.6(16)	B(211)–B(27)	181.7(15)
B(19)–B(18)	175.5(16)	B(29)–B(28)	179.5(16)
B(110)–B(19)	176.4(18)	B(210)–B(29)	178.8(15)
B(111)–B(110)	182.3(16)	B(211)–B(210)	178.7(15)
B(112)–B(111)	174.3(16)	B(212)–B(211)	177.7(15)
B(17)–B(13)	175.7(16)	B(27)–B(23)	184.4(15)
B(15)–B(14)	185.2(17)	B(25)–B(24)	192.3(16)
B(19)–B(14)	172.4(17)	B(29)–B(24)	173.6(16)
B(19)–B(15)	175.4(17)	B(29)–B(25)	174.4(16)
B(110)–B(16)	175.8(16)	B(210)–B(26)	178.5(16)
B(18)–B(17)	179.0(17)	B(28)–B(27)	178.4(15)
B(112)–B(17)	177.7(16)	B(212)–B(27)	176.4(15)
B(112)–B(18)	176.3(17)	B(212)–B(28)	175.5(15)
B(112)–B(19)	175.3(17)	B(212)–B(29)	178.8(16)
B(112)–B(110)	176.1(16)	B(212)–B(210)	178.7(15)
(*ii*) Rhodium to C_5 ring			
C(11)–Rh(12)	220.4(10)	C(21)–Rh(22)	221.2(10)
C(13)–Rh(12)	221.7(11)	C(23)–Rh(22)	223.8(11)
C(15)–Rh(12)	222.1(10)	C(25)–Rh(22)	218.5(10)
C(12)–Rh(12)	222.6(11)	C(22)–Rh(22)	221.5(11)
C(14)–Rh(12)	219.9(10)	C(24)–Rh(22)	222.5(11)
(*iii*) In the C_5 ring			
C(12)–C(11)	143.6(13)	C(22)–C(21)	142.2(13)
C(16)–C(11)	151.6(15)	C(26)–C(21)	147.8(14)
C(17)–C(12)	147.2(14)	C(27)–C(22)	149.4(14)
C(18)–C(13)	150.2(16)	C(28)–C(23)	149.8(15)
C(19)–C(14)	148.2(13)	C(29)–C(24)	150.0(16)
C(15)–C(11)	143.8(13)	C(25)–C(21)	143.6(12)
C(13)–C(12)	144.6(13)	C(23)–C(22)	146.6(13)
C(14)–C(13)	143.7(13)	C(24)–C(23)	141.2(13)
C(15)–C(14)	145.8(13)	C(25)–C(24)	147.0(13)
C(110)–C(15)	146.4(14)	C(210)–C(25)	149.5(14)

Molecule A		Molecule B	
(*iv*) At tellurium			
Rh(12)–Te(11)–B(13)	55.1(4)	Rh(22)–Te(21)–B(23)	55.9(3)
B(13)–Te(11)–B(14)	49.1(4)	B(23)–Te(21)–B(24)	49.4(3)
B(14)–Te(11)–B(15)	48.2(4)	B(24)–Te(21)–B(25)	49.2(4)
B(15)–Te(11)–B(16)	50.2(5)	B(25)–Te(21)–B(26)	49.1(3)
Rh(12)–Te(11)–B(16)	54.8(3)	Rh(22)–Te(21)–B(26)	54.6(3)
(*v*) At rhodium			
Te(11)–Rh(12)–B(13)	59.7(4)	Te(21)–Rh(22)–B(23)	58.9(3)
B(13)–Rh(12)–B(17)	46.2(4)	B(23)–Rh(22)–B(27)	48.0(3)
B(16)–Rh(12)–B(111)	48.1(3)	B(26)–Rh(22)–B(211)	47.8(3)
B(111)–Rh(12)–B(17)	48.5(4)	B(211)–Rh(22)–B(27)	48.5(3)
Te(11)–Rh(12)–B(16)	59.6(4)	Te(21)–Rh(22)–B(26)	59.2(3)
(*vi*) In the RhB_4 ring attached to Te			
B(16)–Rh(12)–B(13)	90.3(5)	B(26)–Rh(22)–B(23)	90.7(4)
Rh(12)–B(13)–B(14)	112.9(7)	Rh(22)–B(23)–B(24)	113.2(6)
B(13)–B(14)–B(15)	111.6(9)	B(23)–B(24)–B(25)	109.9(7)
B(14)–B(15)–B(16)	109.4(8)	B(24)–B(25)–B(26)	109.7(7)
B(15)–B(16)–Rh(12)	113.5(6)	B(25)–B(26)–Rh(22)	115.1(6)
(*vii*) In the TeB_4 ring attached to Rh			
B(13)–Te(11)–B(16)	84.5(4)	B(23)–Te(21)–B(26)	85.9(4)
Te(11)–B(16)–B(111)	113.9(7)	Te(21)–B(26)–B(211)	114.6(6)
B(16)–B(111)–B(17)	111.9(8)	B(26)–B(211)–B(27)	112.7(8)
B(111)–B(17)–B(13)	114.8(8)	B(211)–B(27)–B(23)	113.5(8)
B(17)–B(13)–Te(11)	114.1(7)	B(27)–B(23)–Te(21)	112.8(6)
(*viii*) In the C_5 ring			
C(15)–C(11)–C(12)	109.9(8)	C(25)–C(21)–C(22)	108.1(8)
C(11)–C(12)–C(13)	106.3(9)	C(21)–C(22)–C(23)	108.8(8)
C(12)–C(13)–C(14)	109.4(9)	C(22)–C(23)–C(24)	107.2(9)
C(13)–C(14)–C(15)	107.4(8)	C(23)–C(24)–C(25)	108.5(9)
C(14)–C(15)–C(11)	106.9(8)	C(24)–C(25)–C(21)	107.4(8)

mum deviation of 1.3(8) pm, but the tellurium atom in the TeB_4 face is 22.3(2) and 18.7(2) pm out of the plane containing the four boron atoms for (A) and (B) respectively. The ring C–C bond lengths in (**1**) are all the same within experimental error and this suggests no localisation of the π-electron system. A similar situation is found in, for example, $[\{RhI(\eta^5\text{-}C_5Me_5)\}_2(\mu\text{-}I)_2]$,[9] but in other compounds such as $[RhH(PPh_3)(\eta^5\text{-}C_5Me_5)]PF_6$ the C_5 ring is in an 'ene-enyl' form which has been interpreted as resulting from the large *trans* influence of one of the ligands (H).[10] This type of effect is clearly absent in compound (**1**). In both molecules A and B the methyl groups are directed away from the $RhTeB_{10}$ cage section [mean angle between ring C–C(Me) and C_5 plane is 3.8(5) and 2.8(6)° for (A) and (B) respectively]. The 'staggered' conformation of the C_5 and TeB_4 faces about the rhodium atom, (**IV**), is not unexpected in view of the proposed relative energies and forms of the frontier orbitals of the constituent C_5H_5M[11] and $XB_{10}H_{10}$ fragments.[1] However the 'eclipsed' structure could also have been acceptable and the observed conformation is most probably a result of steric factors. Indeed n.m.r. spectroscopy suggests that the C_5Me_5–M linkage is rotationally fluxional in solution, indicating only small energy differences between eclipsed and staggered forms. The major contributions which are conformation determining in the C_5Me_5–Rh–TeB_4 section of (**1**) can be visualised as shown in Figure 2(*a*) and (*b*). The metal d_{xz} and d_{yz} orbitals interact with the e_1-type ring π orbitals from C_5Me_5 and the highest occupied molecular orbital (h.o.m.o.) and lowest unoccupied molecular orbital (l.u.m.o.) of

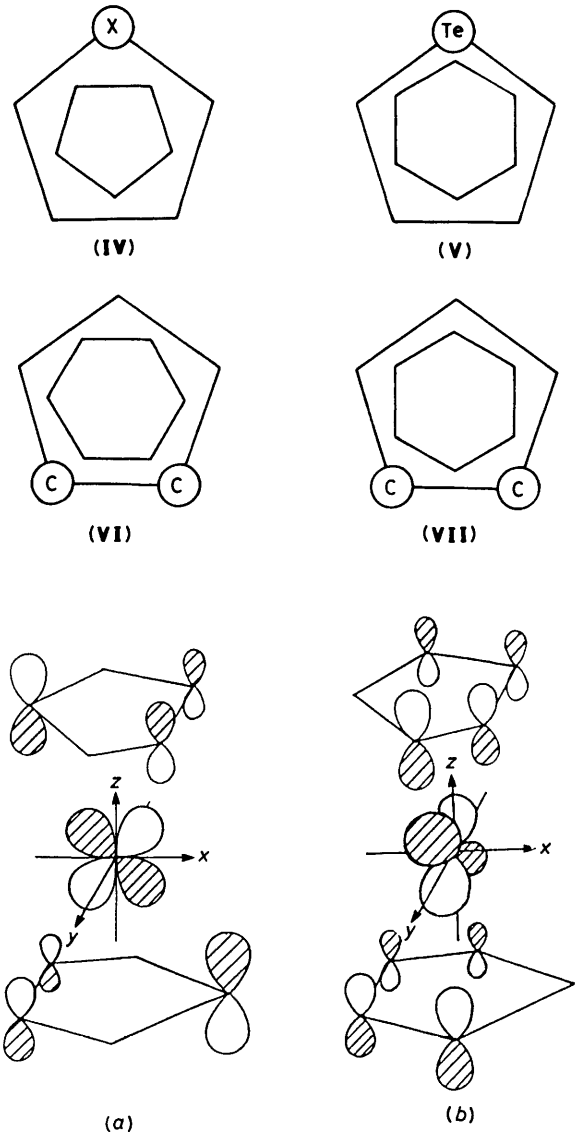

Figure 2. Orbital interaction which determine the conformation of the C_5 and TeB_4 rings around Rh in compound (**1**)

the TeB_{10} species.[1] In general terms, these interactions closely resemble the bonding in the related $[M(\eta^5\text{-}C_5R_5)_2]$ compounds (M = Fe, Ru, or Os) which has been discussed in detail elsewhere.[12]

The only other $(\eta^5\text{-}C_5Me_5)Rh$ containing derivative of a Main Group 6 heteroborane to have been reported previously appears to be the twelve-vertex dimetal species *closo*-$[2,3\text{-}(\eta^5\text{-}C_5Me_5)_2\text{-}7\text{-}Cl\text{-}1,2,3\text{-}SRh_2B_9H_8]$ (**7**).[13] This compound has an icosahedral structure which is more distorted from regular than (**1**) in the heteroatom region [compare the range of Rh–B and Rh–C distances in (**7**), 218.1(6)—231.1(5) and 218.3(5)—229.5(5) pm respectively, with (**1**), Table 1] but less distorted in the borane part of the cage [range of B–B distances in (**7**) 173.7(9)—185.9(7) pm].

Crystals of *closo*-$[2\text{-}(\eta^6\text{-}C_6Me_6)\text{-}1,2\text{-}TeRuB_{10}H_{10}]$ (**3**) suitable for *X*-ray analysis were grown from benzene solution. They were particularly well formed prisms which enabled a data set of excellent quality to be collected. Consequently all the borane hydrogen atoms were readily located in a Fourier difference map and refined without restraint and with isotropic thermal parameters to give the final positions presented here. The cluster

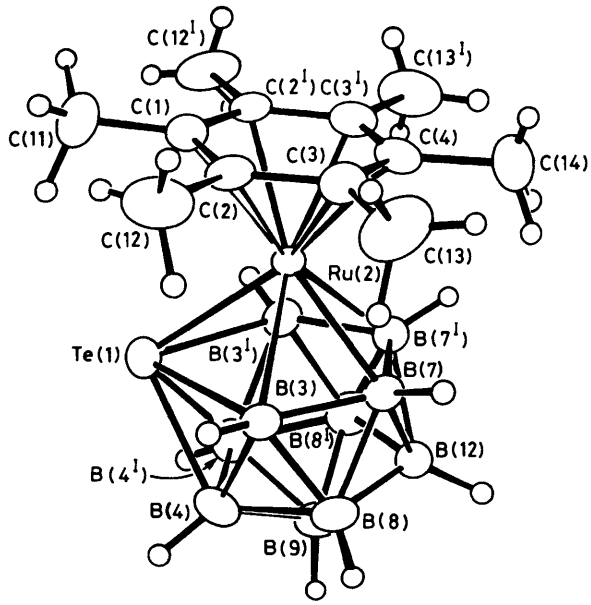

Figure 3. An ORTEP drawing of the molecular structure of *closo*-$[2\text{-}(\eta^6\text{-}C_6Me_6)\text{-}1,2\text{-}TeRuB_{10}H_{10}]$ (**3**)

structure [Figure 3 and (**V**)] possesses crystallographic C_s symmetry [with the mirror plane passing through atoms Te(1), Ru(2), B(9), and B(12)]. As with (**2**) above, it is seen to be based on a triangulated dodecahedron distorted from the regular principally by the incorporation of the relatively large ruthenium and tellurium atoms. Selected molecular dimensions and interatomic angles are given in Table 2. Comparison of compounds (**1**) and (**3**) reveals that in general the dimensions within the cluster cages are very similar with the possible exception of the B(7)–B(7^1) distance in (**3**), 167.5(10) pm, which is significantly shorter than the corresponding B(7)–B(11) distances in the two independent molecules of (**1**) [180.6(16) and 181.7(15) pm]. The ruthenium–tellurium distance in (**3**), 254.9(2) pm, is very close to the rhodium–tellurium distances in the different molecules of (**1**). Whereas in (**1**) there are two distinct sets of Rh–B (or Te–B) distances, in (**3**) the distances between the heteroatoms and boron atoms are much closer, *i.e.* Ru–B 218.9(6) and 221.9(6) pm and Te–B 227.1(7) and 231.0(6) pm respectively.

The bonding in the $(\eta^6\text{-}C_6Me_6)Ru$ section of compound (**3**) is unusual in that there appears to be some localisation of the π-electron density at opposite ends of the C_6 ring which are situated above the tellurium atom and the midpoint of the B(7)–B(7^1) vector, Table 2. This involves distortion of the C_6 ring with atoms C(1) and C(4) further away from the ruthenium atom than C(2) or C(3). Hence the Ru–C distances in (**3**) show a greater range, 218.7(6)—227.6(7) pm, than the corresponding Rh–C distances in (**1**). The determined C(1)–C(2) and C(3)–C(4) distances [135.5(5) and 132.2(6) pm respectively] are significantly shorter than C(2)–C(3) [143.6(6) pm] and the interplanar angle between the plane containing C(2)C(1)C(2^1) and that containing C(2)C(2^1)C(3)C(3^1) is 0.4(4)°. Views of the C_6Me_6–Ru–TeB_4 bonding interactions which determine the conformation in this region of the molecule are given in Figure 4 and there are clear similarities with the C_5Me_5–Rh–TeB_4 case, Figure 2. The structural evidence in Table 2 suggests that in compound (**3**) the interaction in Figure 4(*a*) is the predominant one for metal–heteroborane cage bonding whereas the interaction in Figure 4(*b*) is more important for the metal–C_6 ring bonding. These provide relatively stronger Ru–Te and weaker Ru–C(1) and Ru–C(4) bonding on the one hand [Figure 4(*a*)], and weaker Ru–B(3), Ru–B(7) but stronger Ru–C(2), Ru–C(3)

Table 2. Selected interatomic distances (pm) and angles (°) for compound (3)

(*i*) In the $RuTeB_{10}H_{10}$ cage			
Ru(2)–Te(1)	254.9(2)		
B(4)–Te(1)	227.1(7)	B(3)–Te(1)	231.0(6)
B(3)–Ru(2)	221.9(6)	B(7)–Ru(2)	218.9(6)
B(4)–B(3)	194.9(8)	B(7)–B(3)	174.9(8)
B(8)–B(3)	176.5(8)	H(3)–B(3)	101.9(25)
B(8)–B(4)	173.0(8)	B(9)–B(4)	172.7(9)
H(4)–B(4)	95.9(27)	B(4)–B(4^I)	179.4(12)
B(8)–B(7)	179.8(8)	B(12)–B(7)	176.7(8)
H(7)–B(7)	104.5(25)	B(7)–B(7^I)	167.5(10)
B(9)–B(8)	170.6(8)	B(12)–B(8)	170.3(8)
H(8)–B(8)	90.1(28)	B(12)–B(9)	176.4(11)
H(9)–B(9)	121.9(42)	H(12)–B(12)	118.6(42)
(*ii*) Ruthenium to C_6 ring			
C(1)–Ru(2)	227.6(7)	C(2)–Ru(2)	221.5(5)
C(3)–Ru(2)	218.7(6)	C(4)–Ru(2)	223.1(7)
(*iii*) In the C_6Me_6 ligand			
C(2)–C(1)	135.5(5)	C(11)–C(1)	148.9(9)
C(3)–C(2)	143.6(6)	C(12)–C(2)	142.5(6)
C(4)–C(3)	132.2(6)	C(13)–C(3)	143.7(7)
C(14)–C(4)	153.4(10)		
(*iv*) At Te, Ru and in the TeB(3)B(7)B(7^I)B(3^I), RuB(3)B(4)B(4^I)B(3^I), and C_6 rings			
B(3)–Te(1)–Ru(2)	54.1(2)	Te(1)–Ru(2)–B(3)	57.5(2)
B(3)–Te(1)–B(4)	50.3(3)	B(3)–Ru(2)–B(7)	46.8(1)
B(4)–Te(1)–B(4^I)	46.5(3)	B(7)–Ru(2)–B(7^I)	45.0(2)
B(3)–Te(1)–B(3^I)	80.5(4)	B(3)–Ru(2)–B(3^I)	84.6(2)
Te(1)–B(3)–B(7)	117.4(3)	Ru(2)–B(3)–B(4)	118.8(3)
B(3)–B(7)–B(7^I)	112.7(4)	B(3)–B(4)–B(4^I)	107.8(4)
C(1)–C(2)–C(3)	121.1(5)	C(2)–C(3)–C(4)	122.0(5)
C(2^I)–C(1)–C(2)	116.2(3)	C(3)–C(4)–C(3^I)	117.5(4)

Key to symmetry operation relating designated atoms to reference atoms at (*x*,*y*,*z*): I $x, -y, z$.

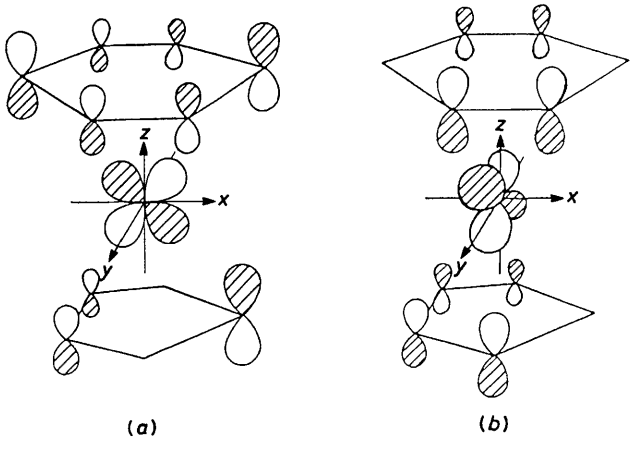

(*a*) (*b*)

Figure 4. Conformation-determining orbital interactions in the C_6–Rh–TeB_4 region of compound (3)

bonding on the other [Figure 4(*b*)]. The 'shortness' of the Ru–Te distance in (3) [or the Rh–Te distance in (1)] compared to the Rh–Te distance in (5) is again noteworthy. Clearly, important synergistic effects are occurring between the cage and *exo*-cage (arene-type) ligands *via* the metal atom. Literature examples of the structural consequences of these effects include the observation of both 'eclipsed' and 'staggered' conformations

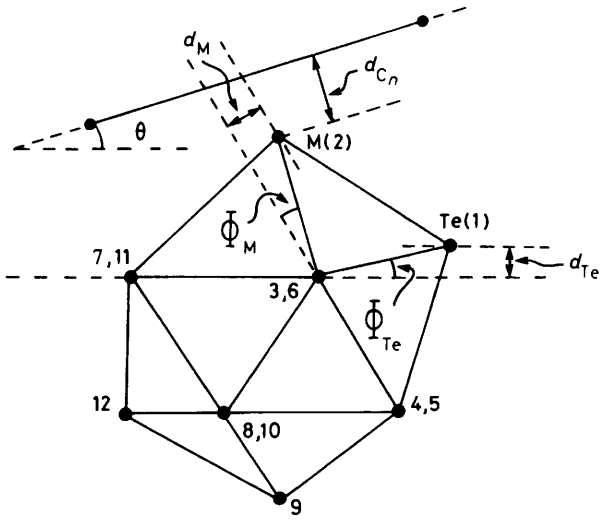

(VIII)

of rings and cages even in the same molecular species, and distortions of metal–ring distances and the distances within rings (see n.m.r. discussion below). For instance, Grimes and co-workers[14] have reported the preparation and molecular structures of [1-(η^6-arene)-2,3-Et_2-1,2,3-$FeC_2B_4H_4$] complexes with η^6-arene = C_6H_6, 1,3,5-$Me_3C_6H_3$, or C_6Me_6. These compounds showed (*a*) both conformations (**VI**) (C_6H_6, $Me_3C_6H_3$) and (**VII**) (C_6H_6, C_6Me_6), (*b*) significant ring C–C distortions in the case of the η^6-C_6H_6 derivatives only, and (*c*) the Me groups bent towards the iron atom in the mesityl derivative, but in the hexamethylbenzene compound five Me bent slightly towards the iron atom and one away. In the η^6-toluene iron *closo* complexes [1-(η^6-MeC_6H_5)-2,4-Me_2-1,2,4-$FeC_2B_9H_9$] reported by Stone and co-workers[15] and [2-(η^6-MeC_6H_5)-2,1-$FeSB_{10}H_{10}$] reported by Sneddon and co-workers[16] the conformations were as shown in diagrams (**VI**) and (**IV**) respectively and there were no significant distortions in the C_6 rings. However in *nido*-[8-(η^6-MeC_6H_5)-8,7-$FeSB_9H_{11}$] significant distortions in the C_6 ring were reported.[16] As far as ruthenium carbaboranes are concerned, neither *closo*-[3-(η^6-C_6H_6)-3,1,2-$RuC_2B_9H_{11}$][15] nor *nido*-[2-(η^6-C_6H_6)-2,5,6-$RuC_2B_7H_{11}$][17] contained any significant differences in C–C distances in the C_6 rings.

In Ru(η^6-C_6Me_6) organometallic chemistry both non-distorted and distorted η^6-C_6 rings have been reported, for example in [Ru(η^6-C_6Me_6)(η^4-cot)] (cot = cyclo-octatetraene)[18] and [Ru(η^6-C_6Me_6)(η^4-C_6Me_6)][19] respectively. It is worth noting in the context of the foregoing discussion that most (if not all) of the *X*-ray structural determinations were carried out at room temperature. However, in the case of [$Cr(CO)_3$(η^6-C_6Me_6)] the structure at 25 °C was reported to contain a non-distorted C_6Me_6 ligand, but a redetermination at 177 K has shown that small but significant distortions are present in the C_6 ring.[20] Hence this gives us confidence in proposing that the distortions in the C_6–Ru region of (3) are significant to the bonding in the Ru–TeB_4 region and *vice versa*.

Other structural features of note in compounds (1) and (3) concern the disposition of the C_n ring–M fragments above the TeB_4 face. Diagram (**VIII**) illustrates these effects and Table 3 gives the relevant data. In both (1) and (3) the C_n ring is tilted away from the tellurium atom with the tilt angle θ of 8.8(2)° for (3), slightly larger than for (1) [mean 7.9(4)°]. Comparison of the other dimensions shows the values for (3) generally fall between those for the two molecules of (1) except for the distance between the metal and (*a*) the centre of the C_n ring, and (*b*) the B(3)B(6)B(7)B(11) plane. In these cases the ruthenium

Table 3. Selected comparative dimensions for compounds [2-(η-C_nMe_n)-1,2-$TeMB_{10}H_{10}$] [M = Rh, (1); Ru, (3)], see (VIII)[a]

Dimension[b]	Ru	Rh (A)	Rh (B)
θ, Angle between planes containing C_n ring and atoms B(3)B(6)B(7)B(11)	8.8(2)	8.0(4)	7.8(3)
Φ_{Te}, Angle between planes containing TeB(3)B(6) and B(3)B(6)B(7)B(11)	6.5(2)	7.2(4)	6.2(4)
Φ_M, Angle between planes containing MB(3)B(6) and B(3)B(4)B(5)B(6)	12.7(1)	13.6(4)	10.2(4)
d_{Te}, Distance of Te from B(3)B(6)B(7)B(11) plane	20.0(2)	22.3(2)	18.7(2)
d_M, Distance of M from B(3)B(4)B(5)B(6) plane	36.1(2)	37.8(3)	28.5(3)
d_{C_n}, Nearest distance of M from C_n plane	174.3(2)	184.2(2)	184.4(2)
Nearest distance of M from B(3)B(6)B(7)B(11) plane	159.7(2)	155.8(2)	155.6(2)
Nearest distance of Te from B(3)B(4)B(5)B(6) plane	166.0(2)	166.7(3)	165.7(3)

[a] B atom numbers refer to compound (1), see (II). The related planes in compound (3) are B(3)B(7)B(7[I])B(3[I]) ≡ B(3)B(6)B(7)B(11), B(3)B(4)B(4[I])B(3[I]) ≡ B(3)B(4)B(5)B(6), TeB(3)B(3[I]) ≡ TeB(3)B(6), and MB(3)B(3[I]) ≡ MB(3)B(6). [b] All angles in ° and distances in pm.

Table 4. Measured n.m.r. parameters for *closo*-[2-(η⁵-C_5Me_5)-1,2-$TeRhB_{10}H_{10}$] (1), *ca.* 0.07 mol dm^{-3} in CD_2Cl_2 (δ in p.p.m., T_1 in ms, ^1J in Hz)

Assignment and relative intensity[a]	δ(^{11}B) (298 K)[b]	Observed [^{11}B–^{11}B]-COSY[c,d] correlations (298 K)	T_1(^{11}B) (approx.) (298 K)	^1J(^{11}B–^{1}H)[e] (298 K)	δ(^{1}H)[f,g] (303 K)	Observed [^{1}H–^{1}H]-COSY[h,d] correlations (303 K)
(12) (1B)	+14.3	(9)m, (8,10)s[i]	*ca.* 10[j]	*ca.* 141[k]	+5.01	(7,11)s, (9)w, (8,10)m
(7,11) (2B)	+14.6	(3,6)m, (8,10)s[i]	13.9	*ca.* 141[k]	+3.28	(12)s, (3,6)m, (4,5)w?, (8,10)s
(9) (1B)	+4.9	(12)m, (4,5)w, (8,10)s	8.0	153	+4.79	(12)w, (4,5)m, (8,10)m
(3,6) (2B)	+6.4	(7,11)m, (8,10)m	5.1	159	+2.84	(7,11)m, (4,5)w, (8,10)w?
(4,5) (2B)	−18.2	(9)w, (8,10)w	4.2	161	+2.24	(7,11)w?, (3,6)w, (9)m, (8,10)m
(8,10) (2B)	−11.2	(12;7,11)s,[l] (9)s, (3,6)w, (4,5)w	18.4	143	+2.92	(12)m, (7,11)s, (9)m, (3,6)w?, (4,5)m

[a] By relative intensities, two dimensional [^{1}H–^{1}H]-COSY and [^{11}B–^{11}B]-COSY cross-peaks, and parallels with the [$(PPh_3)_2HRhTeB_{10}H_{10}$] analogue (ref. 6). [b] ±0.5 p.p.m. to high frequency (low field) of $BF_3(OEt_2)$ in $CDCl_3$. [c] Measured with {^{1}H(broad-band noise)} decoupling. [d] s = Strong, w = weak, and m = intermediate. [e] ±8 Hz measured from ^{11}B n.m.r. spectrum with resolution enhancement to achieve baseline separation of doublet components. [f] ±0.05 p.p.m. to high frequency of $SiMe_4$; δ(^{1}H) assigned to directly bound B atoms by ^{1}H-{^{11}B(selective)} experiments. [g] δ(^{1}H)(C_5Me_5) +2.01 [d, ^3J(^{103}Rh–^{1}H) 1.5 ± 0.1 Hz]. [h] Measured with {^{11}B(broad-band noise)} decoupling. [i] Any ^{11}B(12)–^{11}B(7,11) correlation not observable due to near-coincidence of the ^{11}B resonances. [j] Estimated from τ_{null} value in an 180-τ-90 inversion recovery experiment; ^{11}B(12) resonance partially obscured by ^{11}B(7,11) resonance. [k] Approximate value; near-coincidence of ^{11}B(12) and ^{11}B(7,11) precludes greater accuracy. [l] Individual correlations to ^{11}B(12) and ^{11}B(7,11) not differentiated.

Table 5. Measured n.m.r. data for [2-(η⁶-*p*-$MeC_6H_4Pr^i$)-1,2-$TeRuB_{10}H_{10}$] (2) and [2-(η⁶-C_6Me_6)-1,2-$TeRuB_{10}H_{10}$] (3)

		Compound (2)		Compound (3)	
Assignment	Relative intensity	δ(^{11}B)[a]	δ(^{1}H)[b]	δ(^{11}B)[a]	δ(^{1}H)[b]
(12)	1BH	+12.9	+4.89	+13.0	+4.82
(7,11)	2BH	+7.7	+3.47	+10.5	+2.80
(3,6)	2BH	+2.6	+2.72	+5.1	+2.48
(9)	1BH	+6.7	+4.80	+4.2	+4.69
(8,10)	2BH	−12.2	+2.71	−11.9	+2.71
(4,5)	2BH	−20.3	+2.0	−20.3	+1.96
(1)	—	Ru	—[d]	Ru	+2.21[c]

[a] In p.p.m. ±0.5 to high frequency (low field) of $BF_3(OEt_2)$. [b] In p.p.m. ±0.05, to high frequency (low field) of $SiMe_4$; δ(^{1}H) related to directly bound B atom positions in ^{1}H-{^{11}B(selective)} experiments. [c] Refers to η⁶-C_6Me_6 grouping. [d] δ(^{1}H) for η⁶-*p*-$MeC_6H_4Pr^i$ grouping as follows: +2.24 (3 H, s) for Me; +5.99 and +5.88 {4 H, [AX]$_2$ pattern, $|^3J(AX) + {}^5J(AX')| = 6.3$ Hz} for C_6H_4; +2.75 (1 H, spt, splitting 6.7 Hz) and +1.26 (6 H, d, splitting 6.7 Hz) for Pr^i.

atom is closer to the C_n ring and further from the B_4 plane. We consider that the tilting of the C_n rings away from the tellurium atom is principally a consequence of the difference in the atomic sizes of Te and B and not a result of 'slippage' of the (η-ligand)M fragment.

The measured n.m.r. parameters for the rhodatelluraborane (1) and for the two ruthenatelluraboranes (2) and (3) are given in Tables 4 and 5. These were all consistent with the established [(1) and (3)] and proposed [compound (2)] structures. We discuss in detail the spectroscopy involved in the assignments for the rhodatelluraborane (1). The behaviour for compounds (2) and (3) was almost exactly analogous.

For compound (1) the 1:2:1:2:2:2 relative intensity pattern in each of the ^{11}B and ^{1}H n.m.r. spectra is confirmatory of the symmetrical closed configuration, as is the absence of bridging ^{1}H resonances. The spectra are assigned to the structure on the basis of relative intensities and two-dimensional correlation spectroscopy (COSY) correlations (Table 4), the chosen alternative of the two possible assignments that result from this being selected on the basis of (*a*) shielding parallels with the recently reported *closo*-[2,2-$(PPh_3)_2$-2-H-1,2-$TeRhB_{10}H_{10}$] analogue (5),[6] together with (*b*) the absence of an ^{11}B(3,6)–^{11}B(4,5) correlation flanking the electronegative Te(1) heteroatom; this latter feature is characteristic of the *closo*-{$MTeB_{10}$} structural type.[6,7] It may be noted that the two near-coincident resonances around δ(^{11}B) *ca.* +14.5 p.p.m. are slightly differentiated (*a*) in their [^{11}B–^{11}B]-COSY correlations [specifically ^{11}B(9) *versus* ^{11}B(3,6)], and (*b*) in the results of ^{1}H-{^{11}B(selective)} experiments that produce small but specific differential sharpening effects on the two ^{1}H

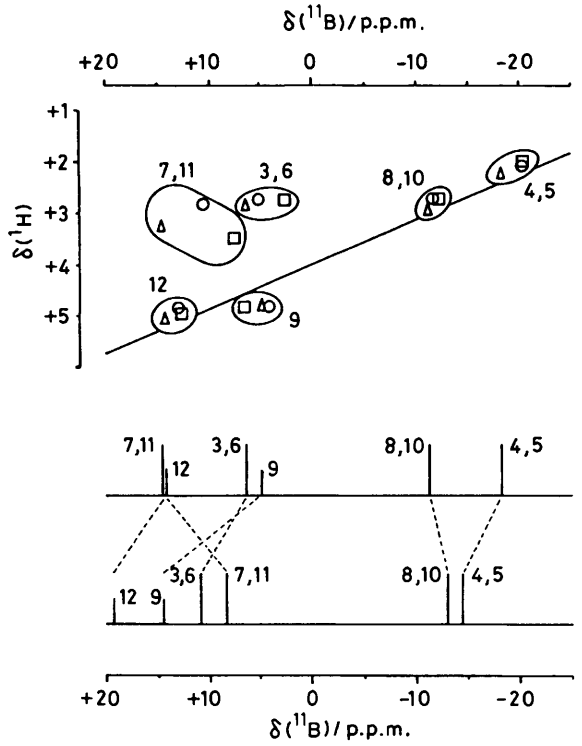

Figure 5. The uppermost diagram is a plot of $\delta(^{11}B)$ *versus* $\delta(^{1}H)$ for directly bound atoms in [2-(η^5-C_5Me_5)-1,2-$TeRhB_{10}H_{10}$] (**1**) (△), [2-(η^6-*p*-$MeC_6H_4Pr^i$)-1,2-$TeRuB_{10}H_{10}$] (**2**) (□), and [2-(η^6-C_6Me_6)-1,2-$TeRuB_{10}H_{10}$] (**3**) (○). The line drawn has slope $\delta(^{11}B):\delta(^{1}H)$ 11.5:1 and intercept $\delta(^{1}H)$ +4.00 (compare refs. 1, 6, and 7). The bottom diagram consists of stick representations of the relative intensities and chemical shifts in the ^{11}B n.m.r. spectra of compound (**1**) and its phosphine-ligated analogue (**5**) (data from ref. 6). The hatched lines join resonances for equivalent positions in the two species

resonances when ^{11}B frequencies on either side of that corresponding to +14.5 p.p.m. are used.

Unlike related platinum species,[17] but in common with (**5**),[6] no coupling to the metal nuclide was apparent for the cluster ^{11}B and ^{1}H n.m.r. resonances. This is expected as coupling to ^{103}Rh is generally at least an order of magnitude less than coupling to ^{195}Pt for equivalent bonding situations.[21] The only instance of measurable ^{103}Rh coupling for compound (**1**) was of *ca.* 1.5 Hz to the C-methyl proton resonance of the η^5-C_5Me_5 ligand, a feature also sometimes observed in η^5-C_5Me_5-containing rhodaboranes that do not contain a heteroatom.[22]

The observed [^{11}B–^{11}B]-COSY correlations for compound (**1**) are very similar, in their incidence and *relative* intensities, to those measured for (**5**)[6] and *closo*-[2,2-$(PEt_3)_2$-1,2-$TePtB_{10}H_{10}$] (**8**),[7] although their observable absolute intensities were somewhat greater which permits correlations to be observed for compound (**1**) which were not apparent for the two phosphine compounds cited. This phenomenon arises from the slower ^{11}B relaxation times for the more compact molecule (**1**). It may be noted that the *relative* ^{11}B relaxation times parallel those reported for the other species,[6,7] which gives additional support to the assignments discussed in the previous paragraphs. The inter-proton correlations are also very similar to the few previously reported for this structural type,[6,7] all arising from $^3J(^1H–^1H)$ paths except for a possible very weak correlation between $^{1}H(4,5)$ and $^{1}H(7,11)$ which if real would be *via* a ^4J pathway.

As mentioned above, the n.m.r. behaviour for the two ruthenium compounds, (**2**) and (**3**) (Table 5), was very similar to that of the rhodium compound (**1**). Figure 5 contains a plot of $\delta(^{11}B)$ *versus* $\delta(^{1}H)$ for directly bound BH units in the three compounds and it can be seen that the (^{1}B, ^{1}H) points fall within closely defined areas for particular structure positions, emphasising the electronic similarities of the three clusters suggested by the very similar geometries discussed above. For all three compounds the ^{1}H n.m.r. properties of the hydrocarbon ligands suggest essentially free rotation of the rings about approximate M(2)–B(9) axes in solution at ambient temperatures.

The bottom diagram in Figure 5 compares the ^{11}B shielding pattern for the rhodium species (**1**) with that previously reported for the phosphine-ligated species (**5**) which is isoelectronic in gross cluster electron-counting terms. The shielding patterns reflect these gross electronic similarities, *i.e.* with the (4,5) and (8,10) shieldings grouped towards higher field, and the (9), (12), (3,6), and (7,11) towards lower, but it is also apparent that the cluster electronic structure is significantly affected by the change in *exo*-polyhedral ligands on the metal. In particular the $^{11}B(9)$ nucleus antipodal to Rh(2) is more shielded by some 10 p.p.m. when the η^5-C_5Me_5 ligand replaces the {$(PPh_3)_2H$} group of ligands, whereas $^{11}B(7,11)$ nuclei adjacent to Rh(2) are significantly deshielded. In this context it is interesting that significant deshielding of adjacent ^{11}B nuclei has also been observed in (η^5-C_5Me_5)Rh *nido* ten-vertex metallaborane systems,[23] and may be associated with the cage to exo-cage synergistic bonding effects mentioned above. However, lack of comparison data precludes a more general assessment of this effect.

Two aspects of the ^{1}H shielding behaviour, $\sigma(^{1}H)$, of compounds (**1**)—(**3**) merit comment. First, although there is a general correlation with the ^{11}B shielding (Figure 5, top diagram), with the relationship being very similar to those that we have previously established for some phosphine-ligated *closo*-2,1-metallatelluradodecaboranes,[6,7] there are two deviations from the general trend. These are the data for the BH(7,11) and BH(3,6) positions, which are some 1.5—2.0 p.p.m. in $\sigma(^{1}H)$ above the general plot. Possibilities to account for this anomalously high proton shielding include (*a*) their being in the 'aromatic' shielding core of the C_nMe_n groups, or (*b*) steric interaction with the C_nMe_n-methyl hydrogen atoms. Some support for the latter explanation derives from the proton shielding behaviour of the phosphine-ligated species (**5**) and (**8**). In these latter compounds only the $^{1}H(3,6)$ protons are anomalously highly shielded, with single-crystal *X*-ray diffraction analysis showing in (**5**) [and suggesting in (**8**)] that these are the positions that are eclipsed by the bulky phosphine organyl groups in the minimum-energy rotamer configuration, the $^{1}H(7,11)$ positions being uncrowded. The second point meriting comment in the context of comparative metallatelluraborane chemistry is that the $^{1}H(9)$ shieldings are not significantly below the general correlation, in accord with their antipodal metal atoms [Ru(2) or Rh(2)] being second-row transition elements. For third-row transition-element *closo*-2,1-$MTeB_{10}H_{10}$ cluster compounds (M = Pt or Ir), the antipodal $^{1}H(9)$ proton is significantly deshielded with respect to the general trend.[6,7]

The major product from the reaction between *nido*-[7-$TeB_{10}H_{11}$]$^-$ and [{$Ru(\eta^6$-$C_6Me_6)Cl_2$}$_2$] in ethanol was readily identified as *nido*-[6-(η^6-C_6Me_6)-8-(OEt)-6-RuB_9H_{12}] (**4**) from n.m.r. spectroscopy. The n.m.r. data are summarised in Table 6 and the overall structure is shown in (**III**). Nine different ^{11}B resonance positions and their shielding pattern suggest a *nido*-monometalladecaboranyl cluster which tended to be confirmed by the presence of four bridging hydrogen atoms. Two of these were at high field (−9 to −10 p.p.m. or so) indicating a configuration with the metal in the 6 position. Selective ^{1}H-{^{11}B} experiments related these to the $^{11}B(5)$ and $^{11}B(7)$ resonances (thereby assigning them as such), and [^{11}B–^{11}B]-COSY n.m.r. spectroscopy thence reasonably assigned the

Table 6. Measured n.m.r. parameters for *nido*-[6-η^6-C_6Me_6)-8-(OEt)-6-RuB_9H_{12}] (**4**) in CD_2Cl_2 solution at 294 K

Assignment	$\delta(^{11}B)^a$/ p.p.m.	Observed [^{11}B–^{11}B]-COSY correlations[b]	$^1J(^{11}B$–$^1H)^c$/ Hz	$\delta(^1H)^d$
(7)	+27.8	(3)w, (2)m	*ca.* 155[e]	+4.41[f]
(8)	+22.3	(3)s, (4)m	—[g]	+1.24 (3 H, q), +3.85 (2 H, t)
(1)	+15.8	(5)w, (3)m, (10)m, (2)w, (4)m	137	+3.56
(5)	+11.8	(1)w, (2)s	*ca.* 155[e]	+3.48[h]
(3)	+6.6	(7)w, (8)s, (1)m, (2)w, (4)vw	137	+3.31
(9)	−7.6	(4)m	*ca.* 155[e]	+2.71
(10)	−14.3	(1)m, (4)m	148	+2.05
(2)	−19.2	(7)m, (1)w, (5)s, (3)s	140	+0.13
(4)	−34.0	(8)w, (1)m, (3)vw, (9)m, (10)m	150	+1.10
(1)	Ru	—	—	+2.28 (18 H)[i]
(5,6)	—	—	—	−9.15[j]
(6,7)	—	—	—	−10.37[j]
(8,9)	—	—	—	−0.56
(9,10)	—	—	—	−2.96

[a] ±0.5 p.p.m. to high frequency of $BF_3(OEt_2)$. [b] Recorded wth {^{1}H(broad-band noise)} decoupling; s = strong, w = weak, m = intermediate, and v = very. [c] Measured from ^{11}B n.m.r. spectrum with resolution enhancement. [d] ±0.05 p.p.m.; $\delta(^1H)$ related to directly bound B positions in ^{1}H-{^{11}B(selective)} experiments. [e] Fine structure (not measured) arising from $^1J[^{11}B$–^1H(bridge)] precludes more accurate estimation. [f] ^{1}H-{^{11}B(selective)} experiments also sharpen $\delta[^1H(6,7)]$. [g] Site of substituent; ^{1}H data refer to 8-ethoxy group. [h] ^{1}H-{^{11}B(selective)} experiments also sharpen $\delta[^1H(5,6)]$. [i] Refers to η^6-C_6Me_6 ligand. [j] See footnotes *f* and *h*.

entire ^{11}B n.m.r. spectrum to the *nido*-6-metalladecaboranyl skeleton, the absence of correlations among the ^{11}B open face 7, 8, 9, 10, and 5 positions being consistent with the weak couplings observed among these positions in *nido* ten-vertex clusters in general.[24–26] The [^{11}B–^{11}B]-COSY cross-correlations were observed for all other connectivities, although there were substantial variations in observed intensities among the different pairs. ^{1}H-{^{11}B(selective)} Spectroscopy showed that all boron atom positions except B(8) had *exo*-terminal hydrogen atoms bound to them. Comparison of the ^{11}B chemical shifts with those[23] of unsubstituted *nido*-[6-(η^6-C_6Me_6)-6-RuB_9H_{13}] indicated a large α-deshielding effect of the order of 20 p.p.m. (Figure 6), indicating hydroxy, oxy, or organyloxy. Chlorine is unlikely as this would probably produce a smaller deshielding effect, although comparison data are limited.[24,27] The presence of apparent CH_3CH_2 resonances in the ^{1}H n.m.r. spectrum, with $\delta(^1H)$ in regions consistent with ethoxy shieldings, suggests that this is due to an 8-ethoxy substituent, (**III**): the differential shielding of the bridging ^{1}H(8,9) and ^{1}H(9,10) nuclei (with that adjacent to the electronegative 8-alkoxy group being some 2.5 p.p.m. to lower shielding) also being generally confirmatory of the assignments and the structural type. It is interesting that large β- and γ-shielding effects of some 13 p.p.m. for ^{11}B(9) and ^{11}B(10) are associated with the ^{11}B(8) α-deshielding effect and there is also a substantial δ-shielding effect at ^{11}B(5) which is 'antipodal'[27,28] to the substituted atom. A plot of $\delta(^{11}B)$ *versus* $\delta(^1H)$ shows a reasonable correlation with a slope $\delta(^{11}B):\delta(^1H)$ 16:1, intercept +2.75 in $\delta(^{11}H)$, but with the $^{11}B^1H(2)$ datum some 1.5 p.p.m. in $\delta(^1H)$ to high field of the correlation line. Both of these features are characteristics of this *nido*-monometalladecaboranyl structural type.[23]

In considering the straightforward ^{11}B n.m.r. spectrum of this compound, it is interesting that its (unassigned) overall appearance is very similar indeed to that of *nido*-[5-(η^6-C_6Me_6)-9-X-5-RuB_9H_{12}] (X = probably OH),[29] which has $\delta(^{11}B)$ +24.4, +20.1, +18.0, +1.5, −10.2, −17.4, −23.6, and −36.4 p.p.m. (all BH doublets, except +18.0 which is a singlet). This emphasises the importance of having additional assignment data (in this case from ^{1}H-{^{11}B(selective)} and [^{11}B–^{11}B]-COSY experiments) in the assessment of structures from spectra.

The formation of the *nido*, ten-vertex non-tellurium-containing, compound (**4**) merits some comment. This compound was formed only when ethanol was used as solvent and not at all when CH_2Cl_2, thf, or benzene was used. The ethanol solvent is implicated in the formation of (**4**) by the presence of the 8-(OEt) substituent. Refluxing the *closo* compound (**3**) in ethanol for 6 h did not lead to the formation of any (**4**) and hence (**4**) is not simply a degradation product of (**3**). The unsubstituted parent compound of (**4**), *i.e.* *nido*-[6-(η^6-C_6Me_6)-6-RuB_9H_{13}], is formed in the reaction of [{$Ru(\eta^6$-$C_6Me_6)Cl_2$}$_2$] with *arachno*-$[B_9H_{14}]^-$ in CH_2Cl_2 solvent,[23] and it may be that ethanolic degradation of the $[TeB_{10}H_{11}]^-$ residue occurs prior to or concomitant with the reaction with the organometallic substrate.

Experimental

General.—All preparative experiments and recrystallisations were carried out in an inert atmosphere. The compounds [{$Rh(\eta^5$-$C_5Me_5)Cl_2$}$_2$],[30] [{$Ru(\eta^6$-arene$)Cl_2$}$_2$] (arene = C_6Me_6 or *p*-$MeC_6H_4Pr^i$),[31] and $Cs[TeB_{10}H_{11}]$[32] were prepared according to literature methods. Infrared spectra were recorded as KBr discs on a Perkin-Elmer 682 spectrometer.

Reactions.—[{$Rh(C_5Me_5)Cl_2$}$_2$] *and* $Cs[TeB_{10}H_{11}]$. Degassed ethanol (60 cm^3) was added to a mixture of [{$Rh(\eta^5$-$C_5Me_5)Cl_2$}$_2$] (0.088 g, 0.144 mmol) and $Cs[TeB_{10}H_{11}]$ (0.1085 g, 0.286 mmol). The mixture was stirred for 48 h. The blackish yellow precipitate was filtered off. Crystallisation of the precipitate from CH_2Cl_2 solution yielded yellow crystals of [2-(η^5-C_5Me_5)-1,2-$TeRhB_{10}H_{10}$] (0.090 g, 65.0%) (Found: C, 24.55, H, 5.05. $C_{10}H_{25}B_{10}RhTe$ requires C, 24.80; H, 5.15%). I.r.: $\nu_{max.}$ 2 965w, 2 945w, 2 900m, 2 840w, 2 542s (BH), 2 520s (BH), 2 498w (BH), 2 482vs (BH), 2 465m (BH), 1 472w, 1 455s, 1 440m, 1 415m, 1 392w, 1 375s, 1 368w, 1 353w, 1 065m, 1 020m, 1 000vs, 990w, 920w, 895w, 878s, 860m, 848m, 830w, 805m, 760m, 715s, 695w, and 672m cm^{-1}.

[{$Ru(\eta^6$-*p*-$MeC_6H_4Pr^i)Cl_2$}$_2$] *with* $Cs[TeB_{10}H_{11}]$. A solution of $Cs[TeB_{10}H_{11}]$ (0.10 g, 0.26 mmol) and [{$Ru(\eta^6$-*p*-$MeC_6H_4Pr^i)Cl_2$}$_2$] (0.081 g, 0.13 mmol) were stirred in CH_2Cl_2 (60 cm^3) solution for 48 h. The solution was filtered and solvent removed under reduced pressure (rotary film evaporator 25 °C). The crude product was purified by preparative t.l.c. using 100% CH_2Cl_2 as eluant. The major product was recrystallised from CH_2Cl_2–hexane (3:1) to give yellow needles, [2-(η^6-1-Me-4-Pr^i-C_6H_4)-1,2-$TeRuB_{10}H_{10}$] (0.05 g) (40% yield). I.r.: $\nu_{max.}$ 2 962w, 2 953w, 2 921w, 2 897w, 2 543vs (BH), 2 519s (BH), 2 478s (BH), 2 448m (BH), 1 481w, 1 465w, 1 384w, 1 010s, 887w, 866w, 760w, and 720w cm^{-1}.

[{$Ru(\eta^6$-$C_6Me_6)Cl_2$}$_2$] *with* $Cs[TeB_{10}H_{11}]$ *in dichloromethane.* A solution of $Cs[TeB_{10}H_{11}]$ (0.10 g, 0.26 mmol) and [{$Ru(\eta^6$-$C_6Me_6)Cl_2$}$_2$] (0.088 g, 0.13 mmol) were stirred in CH_2Cl_2 (60 cm^3) for 6 d. The solution was filtered and the solvent removed (rotary film evaporator 25 °C). The crude product was purified by preparative t.l.c using 100% CH_2Cl_2 as eluant. The major product [2-(η^6-C_6Me_6)-1,2-$TeRuB_{10}H_{10}$] was recrystallised from benzene as yellow crystals (0.071 g) (60.0% yield). I.r.: $\nu_{max.}$ 2 926w, 2 919w, 2 543s (BH), 2 528vs (BH), 2 504w, 2 497vs (BH), 1 450m, 1 444m, 1 385m, 1 070w, 1 011s, 903w, 889m, 868w, 857w, 770w, 741w, and 680w cm^{-1}.

Table 7. Non-hydrogen atomic co-ordinates ($\times 10^4$) for [2-(η^5-C_5Me_5)-1,2-$TeRhB_{10}H_{10}$] (**1**)

Atom	*x*	*y*	*z*	Atom	*x*	*y*	*z*
Te(11)	1 685.5(6)	9 519.1(4)	8 380.0(2)	C(29)	−1 916(13)	9 985(8)	4 568(4)
Rh(12)	3 351.3(6)	9 237.1(4)	7 695.3(2)	C(210)	−102(12)	8 076(8)	4 452(4)
Te(21)	1 634.4(6)	10 965.1(4)	5 862.4(2)	B(13)	1 116(11)	9 499(7)	7 527(4)
Rh(22)	804.9(6)	9 686.1(4)	5 276.8(2)	B(14)	315(12)	10 487(8)	7 938(4)
C(11)	3 738(9)	7 690(6)	7 792(3)	B(15)	1 616(12)	11 137(7)	8 294(4)
C(12)	4 778(10)	8 210(6)	8 045(3)	B(16)	3 428(11)	10 612(7)	8 137(3)
C(13)	5 491(9)	8 761(6)	7 680(3)	B(17)	2 282(11)	10 105(7)	7 154(4)
C(14)	4 882(9)	8 600(6)	7 212(3)	B(18)	694(11)	10 633(7)	7 318(4)
C(15)	3 794(9)	7 905(6)	7 280(3)	B(19)	980(11)	11 562(7)	7 738(4)
C(16)	2 801(11)	6 957(7)	8 021(4)	B(110)	2 729(11)	11 636(7)	7 860(4)
C(17)	5 103(13)	8 131(8)	8 567(4)	B(111)	3 584(10)	10 753(7)	7 478(4)
C(18)	6 737(12)	9 362(8)	7 757(4)	B(112)	2 151(11)	11 357(8)	7 269(4)
C(19)	5 358(10)	8 998(7)	6 741(3)	B(23)	1 343(10)	11 211(7)	5 007(4)
C(110)	3 007(11)	7 463(8)	6 888(4)	B(24)	3 014(11)	11 720(7)	5 298(4)
C(21)	−75(9)	8 244(6)	5 394(3)	B(25)	3 885(11)	10 739(7)	5 679(4)
C(22)	−639(9)	8 886(6)	5 742(3)	B(26)	2 845(10)	9 553(7)	5 641(4)
C(23)	−1 385(9)	9 639(7)	5 483(3)	B(27)	1 972(10)	10 197(7)	4 639(3)
C(24)	−1 263(9)	9 448(7)	4 980(3)	B(28)	2 928(10)	11 274(7)	4 709(4)
C(25)	−417(9)	8 589(6)	4 917(3)	B(29)	4 371(11)	11 045(7)	5 088(4)
C(26)	692(11)	7 361(7)	5 508(4)	B(210)	4 280(10)	9 814(7)	5 269(4)
C(27)	−571(11)	8 767(7)	6 282(4)	B(211)	2 820(9)	9 279(7)	4 997(3)
C(28)	−2 160(12)	10 451(8)	5 708(4)	B(212)	3 754(10)	10 161(7)	4 672(4)

Table 8. Non-hydrogen atomic co-ordinates ($\times 10^4$) for [2-(η^6-C_6Me_6)-1,2-$TeRuB_{10}H_{10}$] (**3**)

Atom	*x*	*y*	*z*
Te(1)	2 204.3(2)	0*	4 380.5(3)
Ru(2)	1 698.6(2)	0*	2 281.6(3)
C(1)	514(3)	0*	2 550(4)
C(2)	658(2)	1 398(4)	2 043(3)
C(3)	941(2)	1 375(5)	1 022(3)
C(4)	1 068(3)	0*	528(5)
C(11)	203(4)	0*	3 593(6)
C(12)	506(3)	2 888(5)	2 553(4)
C(13)	1 082(3)	2 859(6)	476(5)
C(14)	1 349(4)	0*	−581(6)
B(3)	2 513(2)	1 815(5)	3 096(4)
B(4)	3 315(3)	1 091(6)	4 269(4)
B(7)	2 700(2)	1 019(5)	1 845(3)
B(8)	3 440(2)	1 639(5)	2 944(4)
B(9)	3 900(3)	0*	3 594(5)
B(12)	3 556(3)	0*	2 139(5)

* Co-ordinate fixed on special position.

[{$Ru(\eta^6$-$C_6Me_6)Cl_2$}$_2$] *with* $Cs[TeB_{10}H_{11}]$ *in ethanol.* Degassed absolute alcohol (60 cm^3) was added to a mixture of $Cs[TeB_{10}H_{11}]$ (0.10 g, 0.26 mmol) and [{$Ru(\eta^6$-$C_6Me_6)Cl_2$}$_2$] (0.088 g, 0.13 mmol). The reaction was stirred for 2 d and then refluxed for 1 h. The mixture was filtered and the resulting orange solution concentrated. Preparative t.l.c. using dichloromethane–cyclohexane (80:20) as eluant yielded two products, [2-(η^6-C_6Me_6)-1,2-$TeRuB_{10}H_{10}$] (0.021 g, 14.9%) (**3**) and orange [6-(η^6-C_6Me_6)-8-(OEt)-6-RuB_9H_{12}] (**4**) (0.022 g, 38.2%). I.r.: $\nu_{max.}$ 2 943s, 2 908vs, 2 842s, 2 550m (sh) (BH), 2 520s (BH), 2 498m (sh) (BH), 2 462s (BH), 1 456s, 1 448m, 1 376m, 1 283m, 1 266m, 1 211m, 1 203m, 1 150w, 1 117w, 1 068m, 1 024w, 1 005w, 993m, 871w, 813w, 767w, 719w, 705w, and 666w cm^{-1}.

X-*Ray Diffraction Analyses.*—All crystallographic measurements were made on a Nicolet P3/F diffractometer operating in the ω—2θ scan mode using graphite monochromatised Mo-K_α radiation (λ = 71.069 pm) following a standard procedure described in detail elsewhere.[33] Both data sets were corrected for absorption empirically once their structures had been determined.[34] Both structures were solved *via* standard heavy-atom methods and refined by full-matrix least-squares calculations using the SHELX program system.[35]

For the rhodium complex (which was found to have two molecules in the asymmetric unit) only the rhodium and tellurium atoms were assigned anisotropic thermal parameters with all other non-hydrogen atoms refined with isotropic thermal parameters. Both methyl and borane[8] hydrogen atoms were included in calculated positions and assigned to an overall isotropic thermal parameter (in order to reduce the total number of parameters involved in refinement).

For the ruthenium complex all non-hydrogen atoms were refined with anisotropic thermal parameters. All hydrogen atoms were located in a Fourier difference map. However, the methyl hydrogen atoms were held in fixed positions as they tended to move to unreasonable positions when refined. The borane hydrogen atoms were freely refined with individual isotropic thermal parameters.

In both cases the weighting scheme $w = [\sigma^2(F_o) + g(F_o)^2]^{-1}$ was used at the end of refinement in which the parameter *g* was included in refinement in order to obtain satisfactory agreement analyses. Final non-hydrogen atomic co-ordinates for the rhodium complex (**1**) and ruthenium complex (**3**) are given in Tables 7 and 8 respectively.

Crystal data. Compound (**1**), $C_{10}H_{25}B_{10}RhTe$, M = 483.92, orthorhombic, a = 988.3(1), b = 1 392.6(2), c = 2 745.1(3) pm, U = 3.778 nm^3, Z = 4, space group $P2_12_12_1$, D_c = 1.70 g cm^{-3}, μ = 22.16 cm^{-1}, $F(000)$ = 1 856.

ω Scan widths 2.0° + α-doublet splitting, scan speeds 2.0—29.3° min^{-1} and 4.0 < 2θ < 50.0°. Unique data collected 3 887; observed 3 637 [$I > 1.5\sigma(I)$]. Number of parameters = 229, weighting factor g = 0.0001, R = 0.0364, R' = 0.0397.

Compound (**3**). $C_{12}H_{28}B_{10}RuTe$, M = 509.13, monoclinic, a = 1 850.8(2), b = 882.3(1), c = 1 216.5(1) pm, β = 100.84(1)°, U = 1.9511(4) nm^3, Z = 4, space group $C2/m$, D_c = 1.73 g cm^{-3}, μ = 22.31 cm^{-1}, $F(000)$ = 984.

Data collection parameters as above. Unique data 1 899; observed 1 793 [$I > 2\sigma(I)$]. Number of parameters = 154, weighting factor g = 0.002, R = 0.0286, R' = 0.0403.

Additional material available from the Cambridge Crystallographic Data Centre comprises H-atom co-ordinates, thermal parameters, and remaining bond lengths and angles.

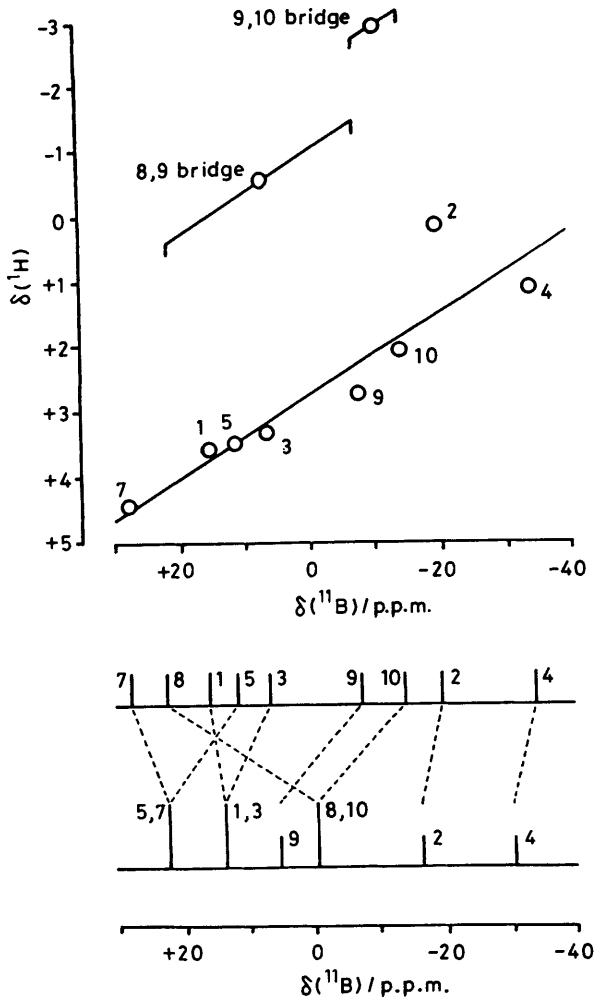

Figure 6. The uppermost diagram is a plot of $\delta(^1H)$ *versus* $\delta(^{11}B)$ for directly bound atoms in *nido*-[6-(η^6-C_6Me_6)-8-(OEt)-6-RuB_9H_{12}] (**4**). The line drawn has slope $\delta(^{11}B):\delta(^1H)$ 16:1 with intercept +2.75 in $\delta(^1H)$ (compare ref. 23). The lower diagram [same scale in $\delta(^{11}B)$] is a stick representation of the chemical shifts and relative intensities in the ^{11}B n.m.r. spectra of (**4**) (upper trace) and its unsubstituted analogue *nido*-[6-(η^6-C_6Me_6)-6-RuB_9H_{13}] (lower trace, data from ref. 23). The lines drawn link resonance positions for equivalent sites in the two compounds

N.M.R. Spectroscopy.—N.m.r. spectroscopy was performed at 9.4 T on commercially available instrumentation, with the general, ^1H-{^{11}B}, COSY, and T_1 techniques being essentially as described and illustrated in other papers in this series.[1,6,7] Chemical shifts δ are given in p.p.m. to high frequency (low field) of Ξ 100 ($SiMe_4$) for ^1H and Ξ 32.083 971 MHz [nominally $BF_3(OEt_2)$ in $CDCl_3$] for ^{11}B, Ξ being defined as in ref. 36.

Acknowledgements

We thank the S.E.R.C. for support and the Department of Education of the Republic of Ireland for Senior Studentships (for F. and M. M.). We thank Professor N. N. Greenwood for his interest in this work. A generous loan of ruthenium and rhodium salts from Johnson Matthey plc is gratefully acknowledged.

References

1 For Part 5, see Faridoon, O. Ni Dhubhghaill, T. R. Spalding, G. Ferguson, X. L. R. Fontaine, and J. D. Kennedy, *J. Chem. Soc., Dalton Trans.*, 1989, 1657.
2 M. Bown, N. N. Greenwood, and J. D. Kennedy, *J. Organomet. Chem.*, 1986, **309**, C67; M. Bown, X. L. R. Fontaine, N. N. Greenwood, J. D. Kennedy, and M. Thornton-Pett, *ibid.*, **315**, C1; M. Bown, X. L. R. Fontaine, N. N. Greenwood, J. D. Kennedy, and P. Mackinnon, *J. Chem. Soc., Chem. Commun.*, 1987, 817; M. Bown, X. L. R. Fontaine, N. N. Greenwood, J. D. Kennedy, and M. Thornton-Pett, *Organometallics*, 1987, **6**, 2254; *J. Chem. Soc., Dalton Trans.*, 1988, 925 and refs. therein.
3 X. L. R. Fontaine, N. N. Greenwood, J. D. Kennedy, P. I. MacKinnon, and M. Thornton-Pett, *J. Chem. Soc., Chem. Commun.*, 1986, 1111; M. Bown, T. Jelínek, B. Štíbr, S. Heřmánek, X. L. R. Fontaine, N. N. Greenwood, J. D. Kennedy, and M. Thornton-Pett, *ibid.*, 1988, 974; M. Bown, H. Fowkes, X. L. R. Fontaine, N. N. Greenwood, J. D. Kennedy, P. MacKinnon, and K. Nestor, *J. Chem. Soc., Dalton Trans.*, 1988, 2597.
4 J. L. Little, G. D. Friesen, and L. J. Todd, *Inorg. Chem.*, 1977, **16**, 869.
5 Faridoon, G. Ferguson, and T. R. Spalding, *Acta Crystallogr., Sect. C*, 1988, **44**, 1371.
6 Faridoon, O. Ni Dhubhghaill, T. R. Spalding, G. Ferguson, B. Kaitner, X. L. R. Fontaine, J. D. Kennedy, and D. Reed, *J. Chem. Soc., Dalton Trans.*, 1988, 2739.
7 G. Ferguson, J. D. Kennedy, X. L. R. Fontaine, Faridoon, and T. R. Spalding, *J. Chem. Soc., Dalton Trans.*, 1988, 2555.
8 A. G. Orpen, *J. Chem. Soc., Dalton Trans.*, 1980, 2509.
9 M. R. Churchill and S. A. Julis, *Inorg. Chem.*, 1979, **18**, 2918.
10 D. M. P. Mingos, P. C. Minshall, M. B. Hursthouse, K. M. A. Malik, and S. D. Willoughby, *J. Organomet. Chem.*, 1979, **181**, 169.
11 M. Elian, M. M. L. Chen, D. M. P. Mingos, and R. Hoffmann, *Inorg. Chem.*, 1976, **15**, 1148.
12 D. M. P. Mingos, in 'Comprehensive Organometallic Chemistry,' eds. G. Wilkinson, F. G. A. Stone, and E. W. Abel, Pergamon, Oxford, 1982, vol. 3, ch. 19.
13 G. Ferguson, M. F. Hawthorne, B. Kaitner, and F. J. Lalor, *Acta Crystallogr., Sect. C*, 1984, **40**, 1707.
14 R. B. Swisher, E. Sinn, and R. N. Grimes, *Organometallics*, 1983, **2**, 506.
15 M. P. Garcia, M. Green, F. G. A. Stone, R. G. Somerville, A. J. Welch, C. E. Briant, D. N. Cox, and D. M. P. Mingos, *J. Chem. Soc., Dalton Trans.*, 1985, 2343.
16 S. O. Kang, P. J. Carroll, and L. G. Sneddon, *Organometallics*, 1988, **7**, 772.
17 T. P. Hanusa, J. C. Huffman, T. L. Curtis, and L. J. Todd, *Inorg. Chem.*, 1985, **24**, 787.
18 M. A. Bennett, T. W. Matheson, G. B. Robertson, A. K. Smith, and P. A. Tucker, *Inorg. Chem.*, 1980, **19**, 1014.
19 G. Huttner and S. Lange, *Acta Crystallogr., Sect. B*, 1972, **28**, 2049.
20 B. P. Byers and M. B. Hall, *Inorg. Chem.*, 1987, **26**, 2186.
21 R. G. Goodfellow, in 'Multinuclear NMR,' ed. J. Mason, Plenum, London, 1987, ch. 20 and refs. therein.
22 See, for example, X. L. R. Fontaine, H. Fowkes, N. N. Greenwood, J. D. Kennedy, and M. Thornton-Pett, *J. Chem. Soc., Dalton Trans.*, 1987, 1437.
23 M. Bown, X. L. R. Fontaine, H. Fowkes, N. N. Greenwood, J. D. Kennedy, P. MacKinnon, and K. Nestor, *J. Chem. Soc., Dalton Trans.*, 1988, 2597; M. Bown, X. L. R. Fontaine, N. N. Greenwood, and J. D. Kennedy, *J. Organomet. Chem.*, 1987, **325**, 233.
24 J. D. Kennedy, in 'Multinuclear NMR,' ed. J. Mason, Plenum, London and New York, 1987, ch. 8 and refs. therein.
25 T. L. Venable, W. C. Hutton, and R. N. Grimes, *J. Am. Chem. Soc.*, 1987, **106**, 29.
26 D. F. Gaines, G. M. Gobvenson, T. G. Hill, and B. R. Adams, *Inorg. Chem.*, 1987, **26**, 1813 and refs. therein.
27 S. Heřmánek, T. Jelínek, J. Plešek, B. Štíbr, J. Fusek, and F. Mareš, in 'Boron (IMEBORON VI),' ed. S. Heřmánek, World Scientific Press, Singapore, 1987, pp. 26—73 and refs. therein.
28 S. Heřmánek, J. Plešek, and B. Štíbr, Abstracts of 2nd International Meeting on Boron Chemistry, Leeds, IMEBORON II, 1974, Abstract no. 38; S. Heřmánek, V. Gregor, B. Štíbr, J. Plešek, Z. Janousek, and V. A. Antonovich, *Collect. Czech Chem. Commun.*, 1977, **41**, 1492.
29 M. Bown, Ph.D. Thesis, University of Leeds, 1987.
30 J. W. Kang, K. Moseley, and P. Maitlis, *J. Am. Chem. Soc.*, 1969, **91**, 5970.

31 M. A. Bennett, T. N. Huang, T. W. Matheson, and A. K. Smith, *Inorg. Synth.*, 1982, **21**, 75.
32 J. L. Little, G. D. Friesen, and L. J. Todd, *Inorg. Chem.*, 1977, **16**, 869.
33 A. Modinos and P. Woodward, *J. Chem. Soc., Dalton Trans.*, 1974, 2065.
34 N. Walker and D. Stuart, *Acta Crystallogr., Sect. A*, 1983, **39**, 158.
35 G. M. Sheldrick, SHELX 76, Program System for *X*-Ray Structure Determination, University of Cambridge, 1976.
36 W. McFarlane, *Proc. R. Soc. London, Sect. A*, 1968, **306**, 185.

Received 1*st August* 1989; *Paper* 9/03254A